Study of bound and resonant states of NS molecule in the R-matrix approach

Study of bound and resonant states of NS molecule in the R-matrix approach

Felix Iacob

West University of Timişoara, 300223 Timişoara, Romania

E-mail: felix.iacob@gmail.com

Thomas Meltzer

Department of Physics and Astronomy, University College London, WC1E 6BT
London, UK

János Zsolt Mezei

Institute for Nuclear Research (ATOMKI), H-4001 Debrecen, Hungary
LOMC, CNRS, Université Le Havre Normandie, 76056 Le Havre, France

E-mail: mezei.zsolt@atomki.hu

Ioan F. Schneider

LOMC, CNRS, Université Le Havre Normandie, 76056 Le Havre, France
LAC, CNRS, Université Paris-Saclay, 91405 Orsay, France

E-mail: ioan.schneider@univ-lehavre.fr

Jonathan Tennyson

Department of Physics and Astronomy, University College London, WC1E 6BT
London, UK
LOMC, CNRS, Université Le Havre Normandie, 76056 Le Havre, France
Institute for Nuclear Research (ATOMKI), H-4001 Debrecen, Hungary
HAS-Distinguished Guest Scientists Fellowship Programme-2022

E-mail: j.tennyson@ucl.ac.uk

Abstract. The bound and resonance states along with corresponding autoionization widths for nitrogen sulphide (NS) molecule are determined using electron NS^+ cation scattering calculations. The calculations are performed for $^2\Sigma^+$, $^2\Pi$ and $^2\Delta$ total symmetries using the *ab initio* R-matrix method for both bound and continuum states. Calculations are performed on a grid of 106 points for internuclear separations between 1.32 and 3 Å. The resonance states yield dissociative potential curves which, when considered together with their widths, provide input for models of different electron-cation collision processes including dissociative recombination, and rotational and vibrational excitation. Curves and couplings which will lead directly to dissociative recombination are identified.

Bound and resonant states of NS molecule   2

Keywords: Diatomic molecules, Rydberg states, Potential energy curves, Resonances, Dissociative recombination

1. Introduction

Sulphur is the tenth and nitrogen is the fifth most abundant element in the Universe, thus their chemistry is of key importance for astronomical environments. It is also known to play a significant role in planetary geochemistry and polymer chemistry. NS emissions are accessible astronomically observation and NS was among the first diatomic molecules to be observed in space [1]. The start of nitrogen sulphide (or more precisely mononitrogen monosulphide) chemistry, dates from the discovery of a compound named as the "thiazyl" radical ($S = N\cdot$) by Demarçay [2]. It was identified inside a polymeric structure $[SN]_x$ known as polythiazyl. Later it was proved that this non-metallic compound has superconducting properties at low temperature and the study of this molecule began to command considerable attention [3].

The situation was not the same for NS^+ cation. Although it is now known to be ubiquitous in the interstellar medium (ISM), it was only recently detected [4]. A year later, the first detection of NS^+ in a photodissociation region of the Horsehead Nebula was reported [5].

A challenge for astrochemistry is to understand mechanisms and rates of formation and destruction of both neutral and cationic molecules. Electrons collisions with cations is a common mechanisms that leads to their dissociation. However, despite its astrochemical importance, no estimate of the dissociative recombination (DR) rate of NS^+ is available [4]. Modelling this mechanism requires the calculation of the doubly excited states of the compound neutral system.

To our knowledge there are no previous studies of e + NS^+ scattering, and relatively few on theoretical studies on the NS^+ target. These studies mostly concern NS electronic ground state. O'Hare [6] performed a self-consistent field (SCF) calculation at the equilibrium geometry, R_e=1.4957 Å, and estimated a dissociation energy of D_0=4.8 eV; Török *et al.* [7] also studied the equilibrium geometry of the X $^1\Sigma^+$ state of NS^+. The low-lying valence states of NS^+ were explored by Karna *et al.* [8] using configuration interaction (CI) calculations. Most important for this work is the more recent study of NS^+ metastable states by Yaghlane and Hochlaf [9].

The purpose of this article is to provide reliable data which can be used as input to models capable of giving good estimates of the DR rate as well as rates for other important processes such as electron-impact vibrational excitation. Our study of electron scattering from the NS^+ cation uses the R-matrix method to give *ab initio* estimates of the bound and continuum states of NS. We identify Feshbach resonances which can provide a route to DR by using a model comprising the ionic core in its ground $X\,^1\Sigma^+$ state and three lowest excited states, a $^3\Sigma^+$, b $^3\Pi$ and c $^3\Delta$. Besides potential energy curves (PEC) of the resonances, we provide their autoionization widths of these doubly excited states; we also provide PECs for bound, singly excited Rydberg states

Bound and resonant states of NS molecule   3

of NS. These Rydberg states are significantly more excited than those computed in the previous study of electronically excited states of NS [10], where only $^2\Sigma^+$ symmetry states were considered. This highly excited Rydberg states of neutral NS provide an important component the DR mechanism for low-energy electron collisions with cations such as those encountered in the ISM.

The article starts with a section detailing our calculations which considers the method, the target model and how our scattering calculations are performed. Section three presents and discusses our results which comprise bound states, resonances, widths and effective principal quantum numbers. Finally, we summarise the main results of this article in the conclusion with pointers towards future work.

2. Calculations

2.1. Method

The R-matrix method is widely used for studies of scattering problems [11]. It was originally formulated for nuclear physics and given an *ab initio* variational formulation for electron collision problems in atomic and molecular physics. A detailed discussion of its application to electron-molecule problems can be found in the extensive review [12].

Our calculations use the UKRmol+ code [13], a new implementation of the time-independent UK R-matrix electron–molecule scattering code, which uses the electronic structure code MOLPRO [14] to provide target wave functions.

The R-matrix method is based on the division of space into an inner and an outer region. The inner region is a sphere, here with radius of 10 a_0, centred on the centre-of-mass of the NS$^+$ target. In the inner region we perform two separate calculations: a target one which considers the N interacting target electrons, and an $N + 1$ electron calculation in which the scattering electron interact with all target electrons. Then these two calculations are used in turn to provide R-matrices on the boundary which are then used in the outer region to calculate scattering properties.

In the inner region the $(N + 1)$-electron system of the target and the colliding electron are described by the wave function:

$$\Psi_k(x_1, \cdots, x_{N+1}) = \mathcal{A} \sum_{i,j} a_{i,j,k} \, \Phi_i^N(x_1, \cdots, x_N) \, u_{i,j}(N + 1)$$
$$+ \sum_i b_{i,k} \, \chi_i^{N+1}(x_1, \cdots, x_{N+1}). \tag{1}$$

Here Φ_i^N are the wave functions describing the ith target state. The $u_{i,j}$ represent the extra continuum orbitals. Φ_i^N and χ_i are constructed to vanish on the R-matrix boundary. Hence, the χ_i, which represent extra configurations obtained by placing the scattering electron in a target orbital, are known as L^2 configurations. The wave funtion of the $N + 1$ electron system has to obey the Pauli principle, which is achieved by the action of $\mathcal{A}$ which represents an anti-symmetrization operator. The coefficients $a_{i,j,k}$ and $b_{i,k}$ are variational coefficients of expansions [15]. To construct the R-matrix on the boundary we used all the solutions of the inner region problem.
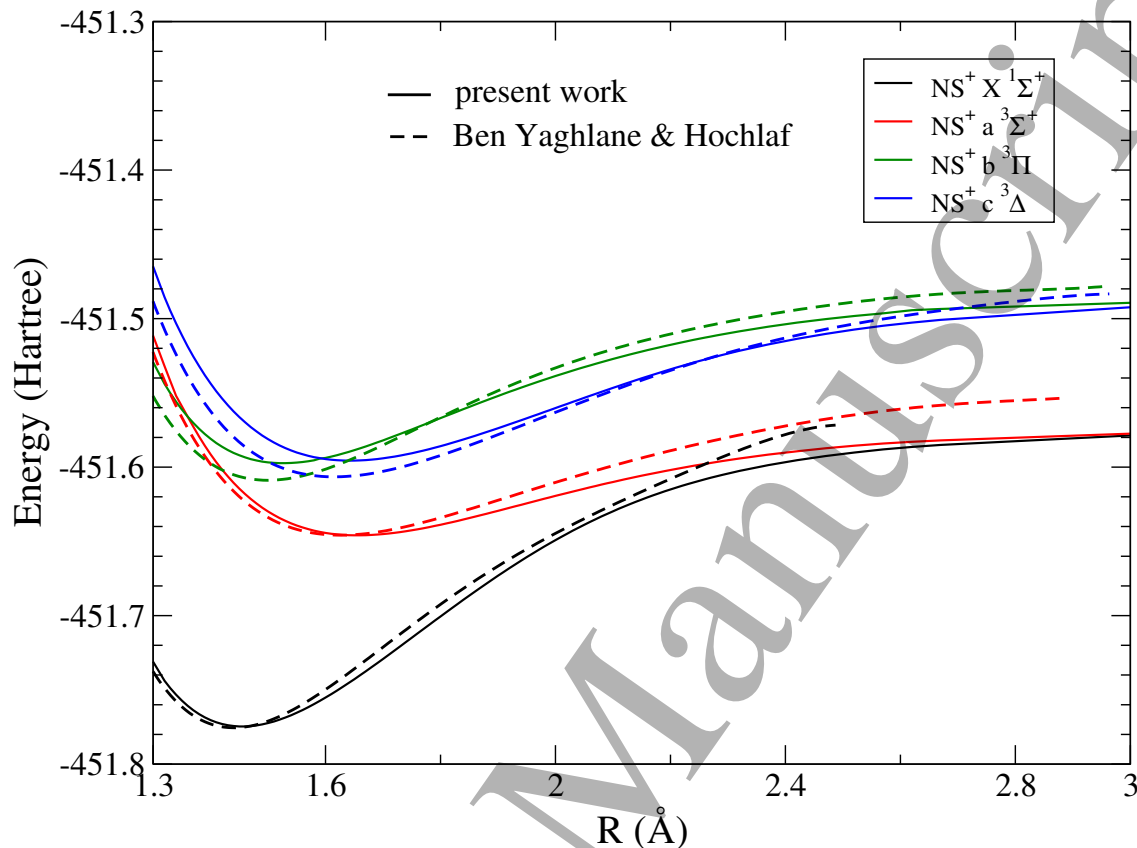
Bound and resonant states of NS molecule　　　　　　　　　　4

Figure 1: Potential energy curves for the ground $(X^1\Sigma^+)$ and three lowest excited states $(a\,^3\Sigma^+, b\,^3\Pi, c\,^3\Delta)$ of NS$^+$ target. Comparison is given with the work of Ben Yaghlane and Hochlaf [9]

Within the framework of the R-matrix method there are a variety of different scattering models and procedures that can be used [12]. Close-coupling (CC) expansions are used here which involves including several target states in Eq. (1). The use of the CC method is essential for describing electronic excitation and is also best for studying Feshbach resonances, which is the major goal of this paper.

2.2. NS$^+$ target

A good description of the target is required when calculating the resonant scattering states of a molecule. A state averaged multi-configuration self-consistent field (MCSCF) model was used to generate the first four states of NS$^+$. These were computed with MOLPRO using a Gaussian type orbital (GTO) cc-pVQZ basis set. Several speed and accuracy tests were performed with different bases to decide the optimal one. The ground state of NS$^+$ is $X\,^1\Sigma^+$ and the equilibrium bond length was determined at 1.44 ± 0.01 Å. The low-lying excited states are all triplets: $a\,^3\Sigma^+$, $b\,^3\Pi^+$ and $c\,^3\Delta^+$.

Bound and resonant states of NS molecule　　　　　　　　　　　　　5

Whilst NS^+ belongs to the $C_{\infty v}$ point group, both MOLPRO and UKRmol+ only allow the calculation to be performed in C_{2v} symmetry. In this case the molecular orbitals are labeled according to their symmetry properties as belonging to one of the four irreducible representations (A_1, A_2, B_1, and B_2). In the case of a linear molecule in the C_{2v} point group, results obtained in the B_1 and B_2 representations are degenerate. The 22 electrons of NS^+ are organized in (10,4,4,1) orbitals of which: (4,1,1,0) are frozen, (4,2,2,0) are used for the complete active space (CAS) and (2,1,1,1) are used as virtual orbitals in the scattering calculation. We note that the fewer frozen orbitals we consider and/or the larger the CAS, the higher accuracy we get but, on the other hand, this high accuracy requires more computer time.

The NS^+ target potential energy curves we obtained are plotted in figure 1. Our calculation is displayed using solid lines and compared with the calculations by Ben Yaghlane and Hochlaf [9], displayed using dashed lines. It can be seen that the agreement with the ground and first excited potential energy curve of the cation is very good. The energy gap between the ground state and first excited state, which is important for determining the positions of the resonance states, is the same in both studies. Slight differences appear for the two higher excited states, b $^3\Pi$, c $^3\Delta$, due to the use of a larger basis set (aug-cc-pV5Z basis set) in [9].

2.3. Scattering calculations

For the scattering calculations we used the NS^+ MCSCF molecular orbitals and target CAS presented in section 2.2, and the same cc-pVQZ basis set. These were supplemented by continuum orbitals $u_{i,j}$ in order to represent the scattering electron. A truncated partial wave expansion around the centre-of-mass with $l \leq 4$ generated as a GTO expansion [16] for an R-matrix radius of 10 a_0. Use of an orthogonalisation deletion threshold of 2×10^{-7} resulted in the removal of (10,6,6,4) orbitals from continuum. The 4 (6 in C_{2v} symmetry) target states shown in Figure 1 were used in the CC model.

Scattering calculations were performed as a function of bondlength, R, on a grid from 1.32 to 2.30 Å with the step 0.01 Å and from 2.30 to 3.0 Å with a step 0.05 Å giving a total of 106 points. Although the C_{2v} point group was used for calculation, results were extracted for $^2\Sigma^+$, $^2\Pi$ and $^2\Delta$ symmetry of the neutral system.

In the outer region the R-matrix were propagated [17] to 150 a_0. Module RESON [18] was used to automatically detect resonances and fit them to a Breit-Wigner profile to determine their position (E_r) and width (Γ) using grids of eigenphase sums computed for each resonance.

3. Results and discussion

In this section we present results for the bound states, and for the autoionizing resonance positions and widths of the neutral NS molecule.

Bound and resonant states of NS molecule   6
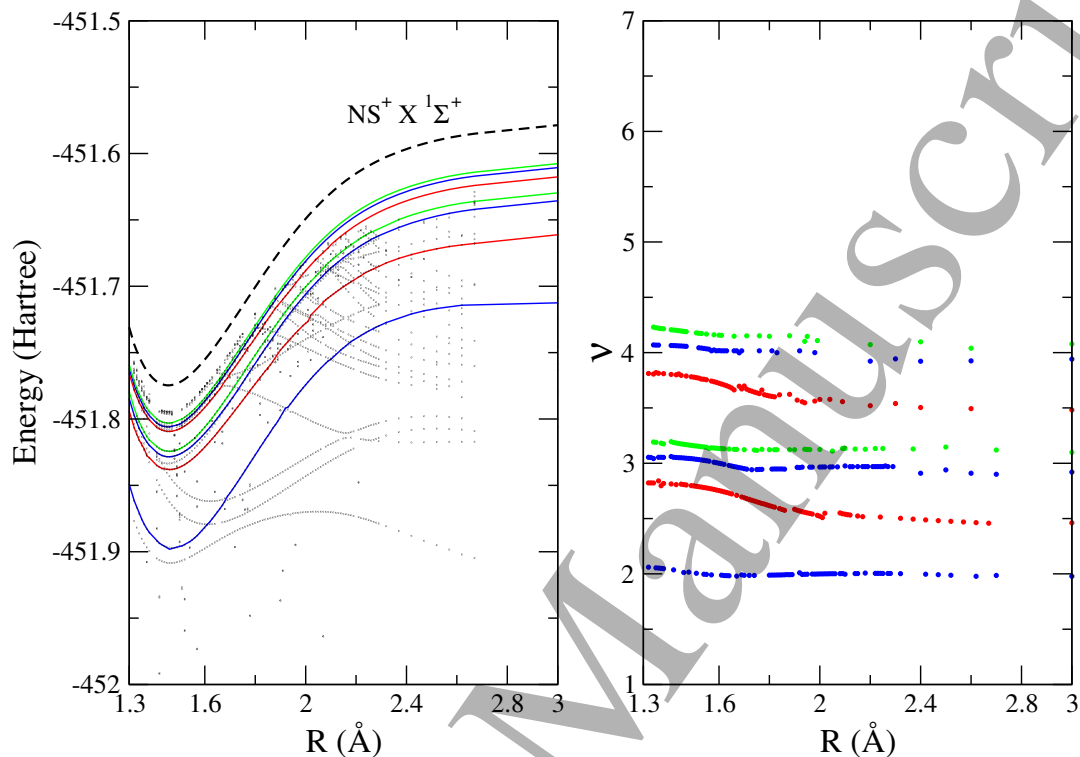

Figure 2: NS $^2\Sigma^+$ bound states: Left panel PECs. Right panel effective principal quantum numbers. Bound states belong to series that converge to $X\,^1\Sigma^+$ symmetry of ion. The partial wave characterizing the Rydberg σ-wave electrons is indicated using colours: blue s, red p, green d.

3.1. Bound states

Bound electronic states of NS where found using the method of Sarpal *et al.* [19]: R-matrices were propagated to 30 a_0 and wave functions computed using an improved Runge-Kutta-Nystrom algorithm [20]. Effective principal quantum numbers (ν) as a function of internuclear separation were calculate from the Rydberg states assuming as threshold of the ground state of the ion.

Bound states were found for $^2\Sigma^+$, $^2\Pi$ and $^2\Delta$ total symmetries. These states are a mixture of Rydberg states which follow the shape of the NS$^+$ X $^1\Sigma^+$ state and valence states which do not. Both sets of states are depicted in our figures. In this section we concentrate characterising the Rydberg series but below we also consider those bound state curves which link with the key, dissociative resonances at large R.

The curves and the effective principal quantum numbers for states we assign as Rydberg-like are shown in figures 2, 3 and 4. In each figure the uppermost dashed black

Bound and resonant states of NS molecule   7

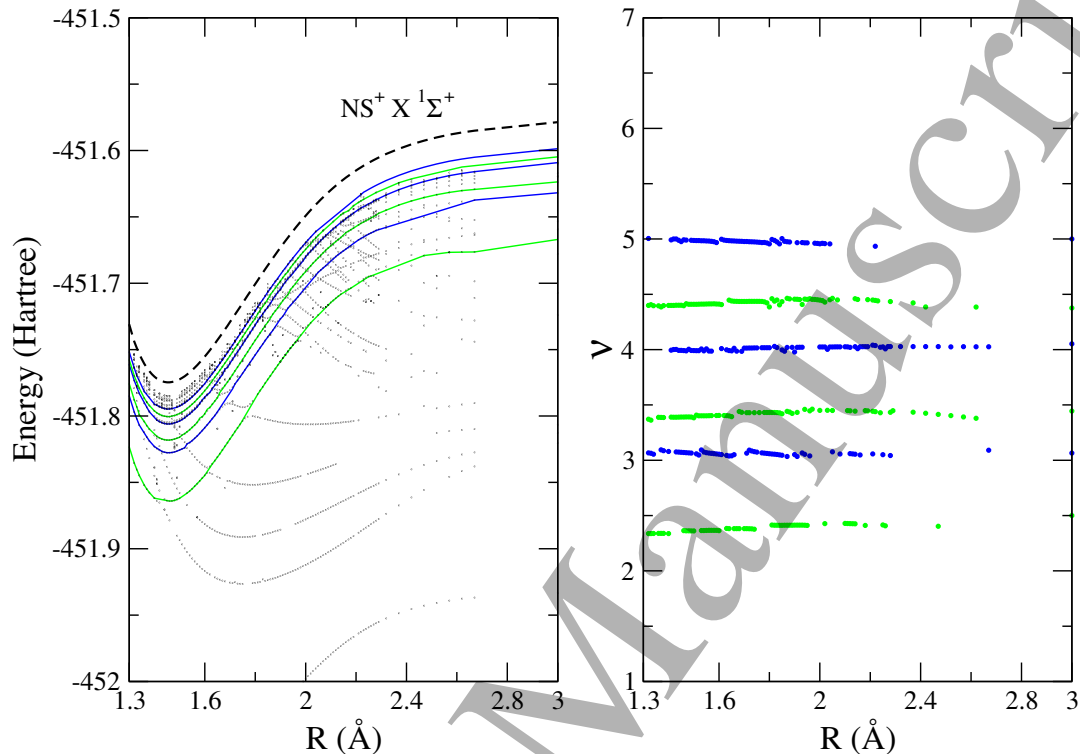Figure 3: NS $^2\Pi^+$, bound states: Left panel PECs. Right panel effective principal quantum numbers. Bound states belong to series that converge to $X\,^1\Sigma^+$ symmetry of ion. The partial wave characterizing the Rydberg π-wave electron is indicated using colours: green p-wave, blue d-wave.

curve gives the $X\,^1\Sigma^+$ ground state of NS$^+$.

If one allocates a dominant partial wave as characterizing the Rydberg electron of each states, one gets different Rydberg series for the various total symmetries. Note our calculations neglect Rydberg series arising partial waves with $\ell > 4$; such states are expected to have quantum defects close to zero. Below we consider the major (i.e. low ℓ) partial waves for each symmetry.

For $^2\Sigma^+$ symmetry we consider s, p and d Rydberg electrons; for $^2\Pi$ symmetry we consider p and d electrons and for $^2\Delta$ symmetry we consider d and f electrons. In general the effective principal quantum numbers of the states show smooth and generally slow variation with R. However, in places the structure of the Rydberg series are complicated by the presence of so-called intruder states which arise from Rydberg series associated with excited states of the ion. Crossings by these intruder states appear as local discontinuities in the ν as a function of R.

Bound and resonant states of NS molecule   8
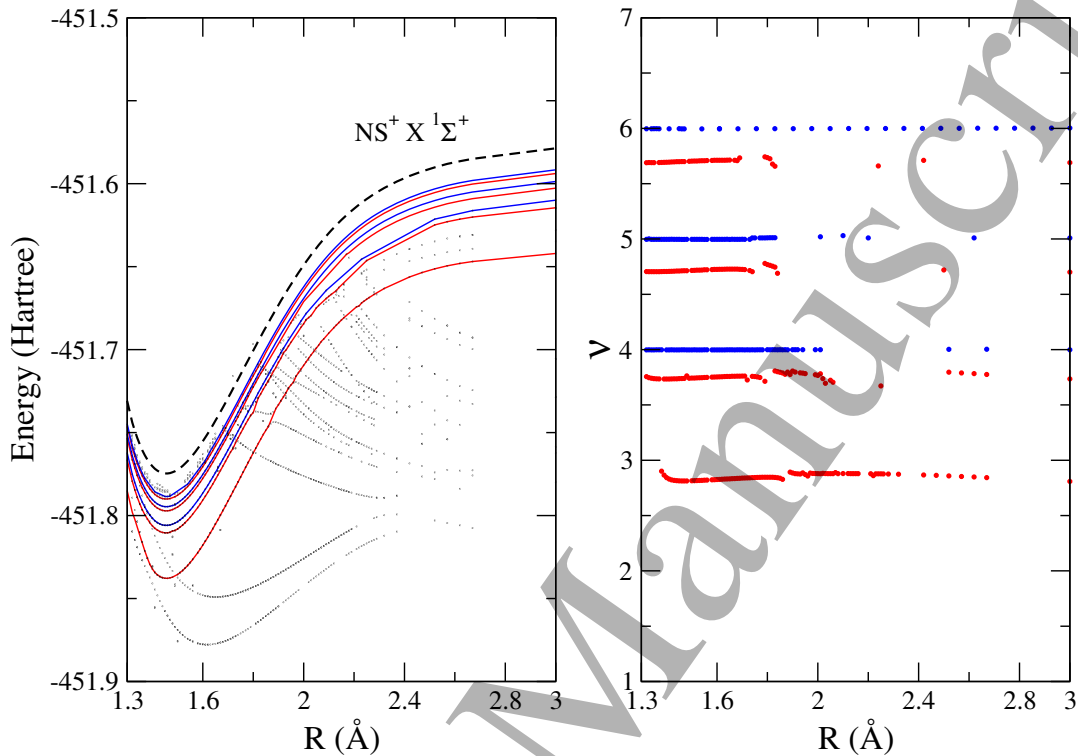

Figure 4: NS $^2\Delta^+$, bound states: Left panel PECs. Right panel effective principal quantum numbers. Bound states belong to series that converge to $X\,^1\Sigma^+$ symmetry of ion. The partial wave characterizing the $\delta - wave$ electron of the states is indicated using colours: red d-wave, blue f-wave.

3.2. Resonance curves

The R-matrix calculation is made in the fixed nuclei approximation and hence the PECs are adiabatic. Resonances were characterised up to approximately 4 eV above the equilibrium energy of the $X\,^1\Sigma^+$ state of ion, which restricts the internuclear distance range to $R \approx 1.2 - 1.8$ Å.

Figures 5, 6, and 7 shows the resonances that are found with emphasis on the PECs that can lead to dissociation as DR occurs along these repulsive PECs. The right panel of each figure shows the real part of the ν for each resonance as a function of R; being derived assuming that the resonance is associated with the first, a $^3\Sigma^+$, excited state. In each figure, the curves can be matched by their colours. Again we concentrate on states of low ℓ as higher ℓ states have quantum defects close to zero and, more importantly, very weak electronic couplings meaning that in general they do not play a significant role in DR.

Bound and resonant states of NS molecule 9

Figure 5 shows that the lowest two curves show almost constant effective principal quantum number for $R > 1.4$ Å. The inflection point at $R = 1.36$ Å is due to the NS$^+$ c$^3\Delta$ curve, which for $R < 1.36$ Å crosses below the a$^3\Sigma$ state. The ν for the highest, black curve in Fig. 5 had to be given special consideration. It showed strong variation with R when taken relative to the a$^3\Sigma^+$ state. Assuming this resonance to be an intruder we plotted its effective principal quantum number relative to both the b$^3\Phi$ and c$^3\Delta$ states but again found strong variations with R. Finally, we took ν relative to the d$^5\Sigma^+$ curve, as calculated by Ben Yaghlane and Hochlaf [9]; this curve is the extra one shown on this figure. This showed much flatter variation although there is a pronounced slope which is possibly caused by the fact that this is not a like-for-like comparison.

The $^2\Pi$ Rydberg states curves presented in figure 6 mostly showing little variation in ν as for $R > 1.4$ Å. However, the $^2\Pi$ symmetry shows avoided crossings between the green with turquoise curves, and the turquoise and blue curves. The approximately constant behaviour of ν with R is maintained with the corresponding change of colours. In the figure 7 the effective principal number shows an inflexion point at $R < 1.36$ Å due to the crossing of NS$^+$ c$^3\Delta$ curve below the a$^3\Sigma$ one. The effective principal number corresponding to the NS** 3 $^2\Delta$ state shows a strong variation with R and a shift at $R = 1.6$ Å. A comparison with a higher excited curve might show an effective quantum number with a flatter dependence on R.

Figure 8 shows the PECs with $^2\Sigma^+$ symmetry of neutral NS in an adiabatic representation. However, following the colours one can see the diabatic states. The curves situated above the PEC of the ion ground state are the resonances and those below it represent bound states. Dissociative PECs of importance for DR comprise of a resonant state in the continuum which cross the ion ground state to become bound states where they then, in the diabatic picture, pass through the Rydberg series associated with the ion ground state. The PECs are smooth except in a vicinity of avoided crossings. Figures 9 and 10 show similar curves for both $^2\Pi$ and $^2\Delta$ symmetry respectively. These curves are the ones which form the input for a model of DR.

3.3. Widths and quantum defects

Complex quantum defects $\mu = \alpha + i\beta$ were obtained from the fitted position and width using the formulae:

$$E_r = E_t - \frac{Ry}{\nu^2}, \quad \Gamma = \frac{2\beta\,Ry}{\nu^3}, \tag{2}$$

where the effective principal quantum number $\nu = n - \alpha$, E_t is the energy of the threshold to which the Rydberg series converges and Ry is the Rydberg constant.

The widths are presented in figure 11 as functions of R; the symmetry is marked on each graph. One may see how the behaviour of widths change when avoided crossings occur. In general, we expect the width of a resonance to decrease as the number of open channels decreases which occurs when a resonances passes through a state of the ion.

Bound and resonant states of NS molecule   10
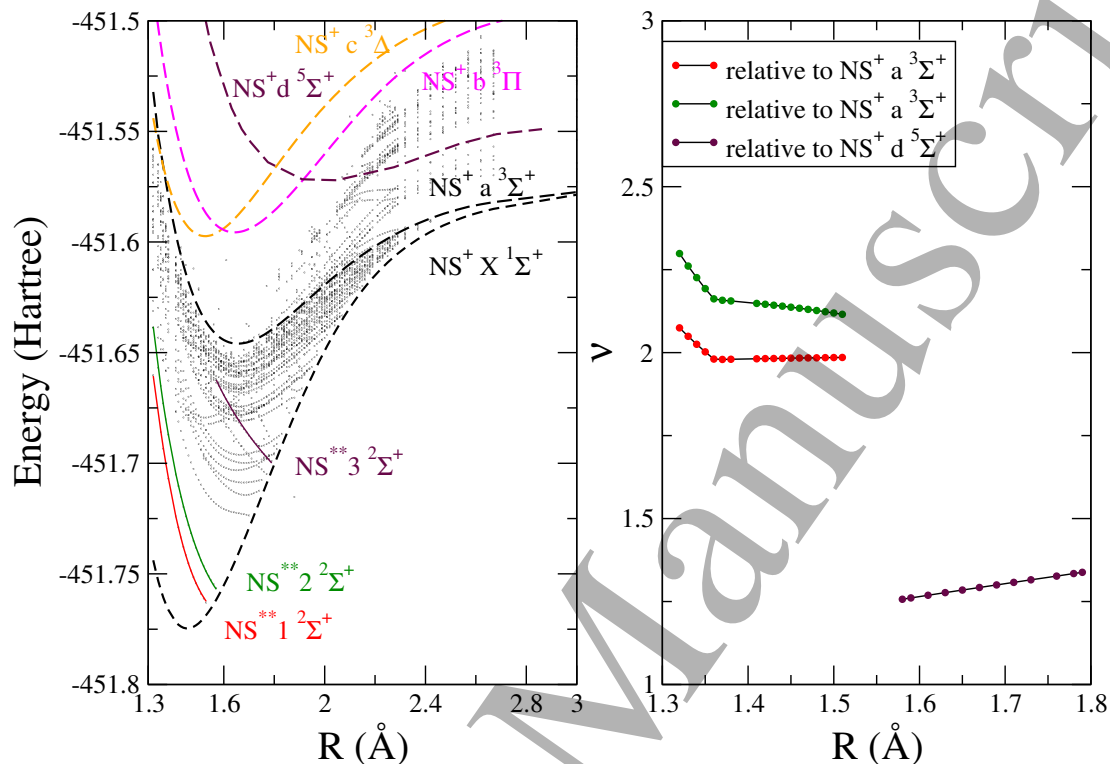

Figure 5: NS $^2\Sigma^+$ symmetry relative to resonances curves (left panel) and effective principal quantum numbers (right panel) for some specific curves of special interest for DR.

Note that the widths should vanish once the resonance states cross the ion ground state and become bound.

4. Conclusions

Resonance positions and auto-ionization widths were calculated for e-NS$^+$ system depending on the internuclear separation. The Rydberg series that converge to ion ground state were computed together with the corresponding effective principal quantum numbers. The use of a dense grid produces numerous resonances and bound states in great details, which facilitate the identification of dissociative states and singly excited Rydberg manifolds. Figures 8, 9, and 10 summarize our results and provide the curves and electronic couplings which will provide the input for future nuclear dynamics (dissociative recombination and ro-vibrational transitions) studies. To our knowledge, this is the first time when relevant molecular data sets were calculated to study electron induced reactive elementary processes in NS$^+$. The data produced in this work will
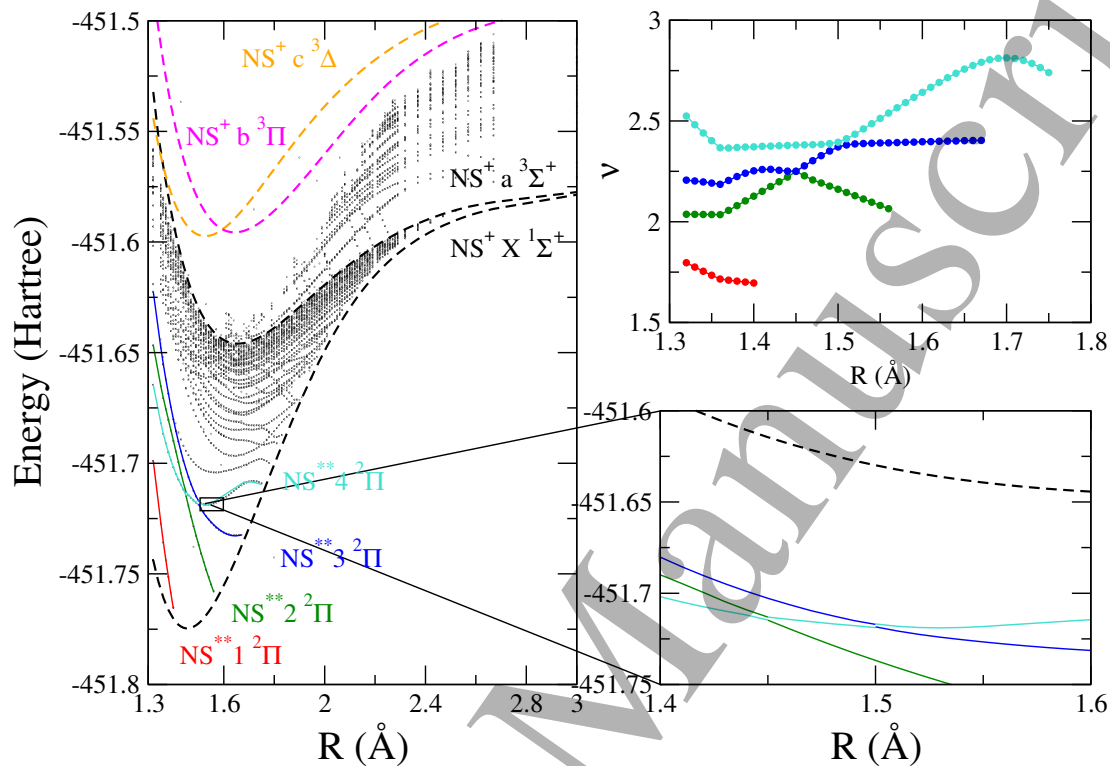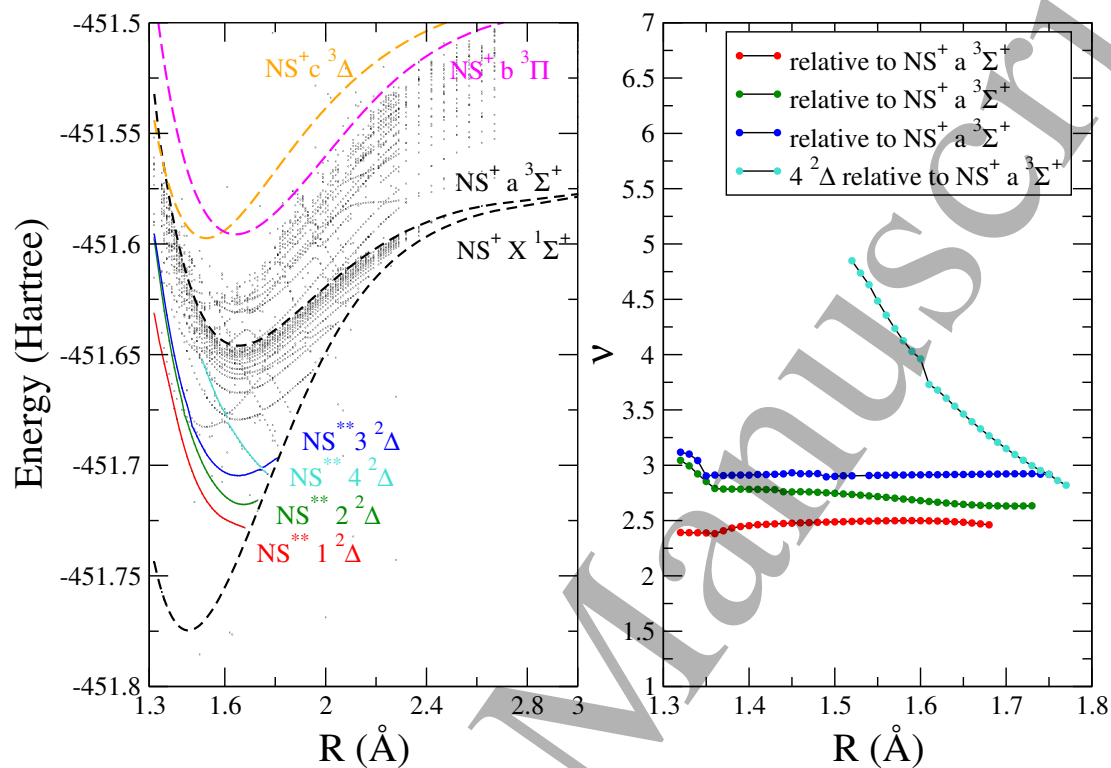
Figure 6: NS $^2\Pi$ symmetry resonances curves (left panel) and effective principal quantum numbers (right panel) for some specific curves of special interest for DR.

be used for calculating dissociative recombination and ro-vibrational transition cross sections and rate coefficients relevant for the astrochemistry of sulphur and nitrogen, using stepwise Multichannel Quantum Defect Theory, that has proven its power for many diatomic and polyatomic molecular systems [21, 22, 23, 24, 25, 26].

Acknowledgments

Bound and resonant states of NS molecule   12

Figure 7: NS $^2\Delta$ symmetry resonances curves (left panel) and effective principal quantum numbers (right panel) for some specific curves of special interest for DR.

Figure 8: NS resonance and the bound states extension for the $^2\Sigma^+$ molecular symmetry as a function of internuclear distance.
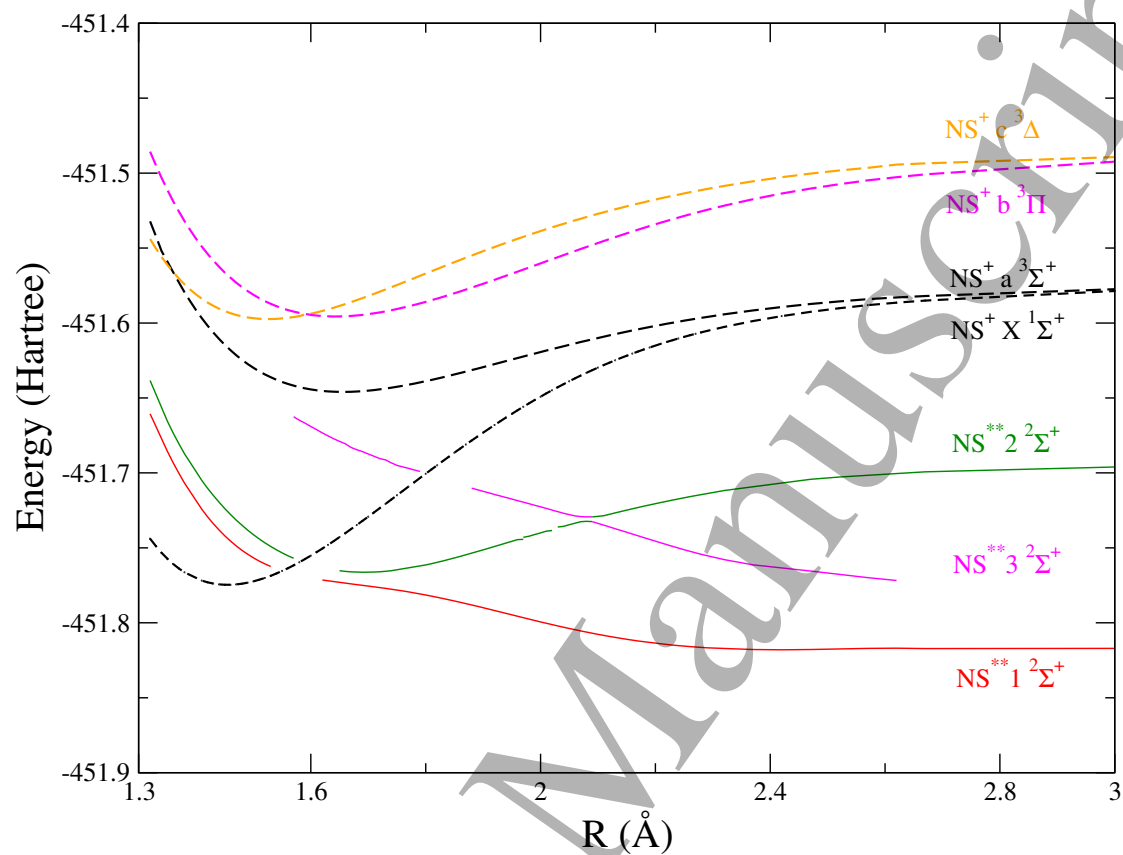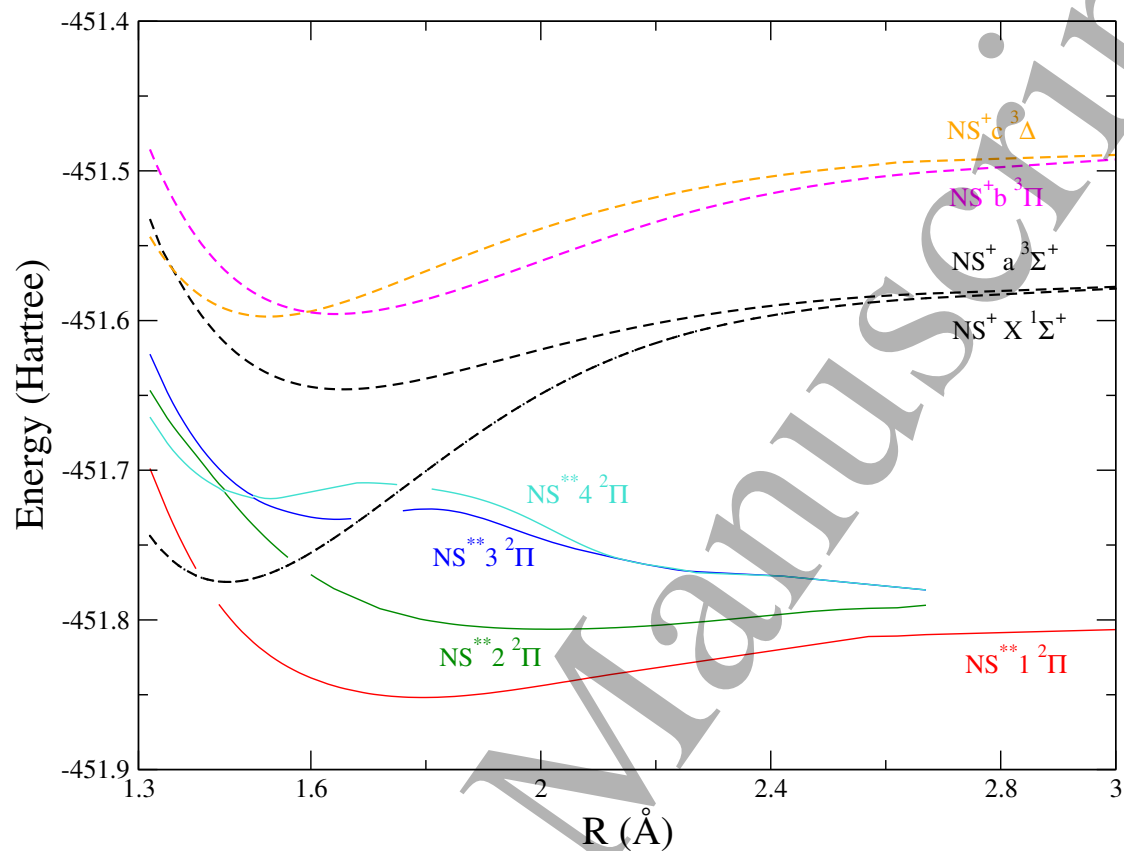
Figure 9: NS resonance and the bound states extension for the $^2\Pi$ molecular symmetry as a function of internuclear distance.
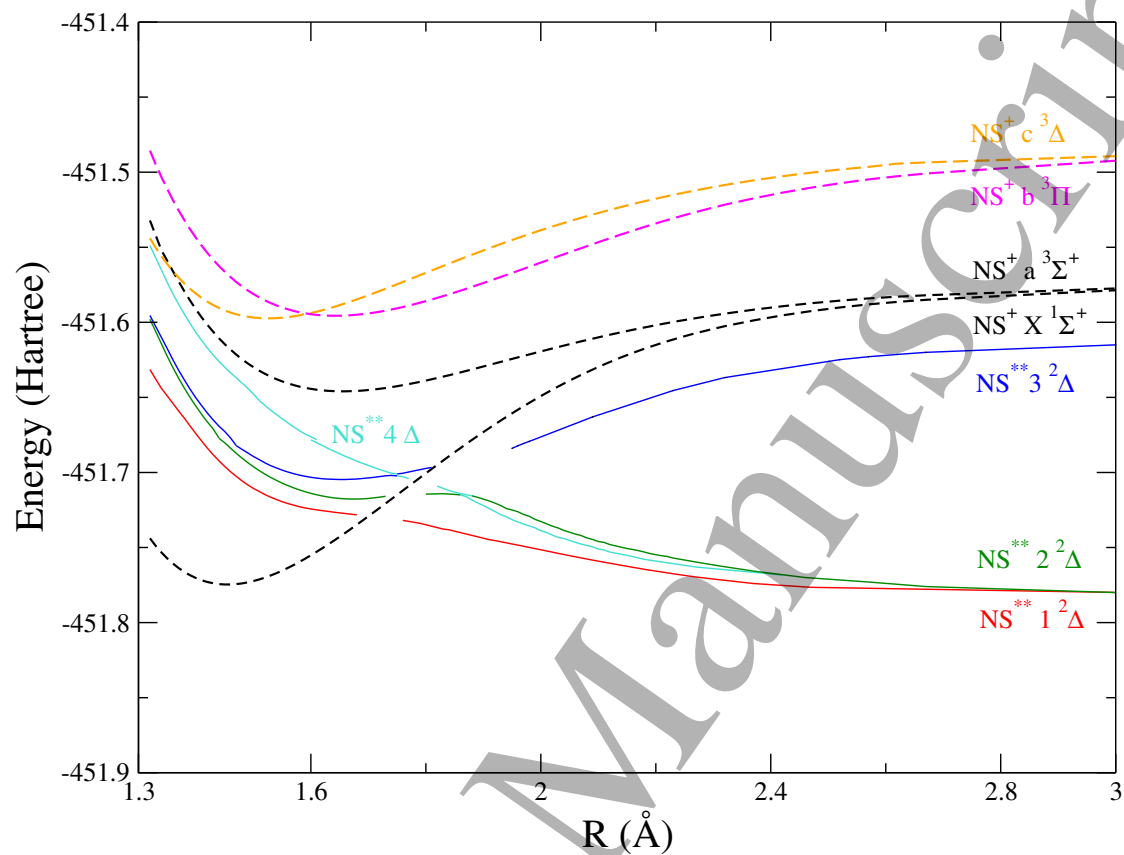
Bound and resonant states of NS molecule 15

Figure 10: NS resonance and the bound states extension for the $^2\Delta$ molecular symmetry as a function of internuclear distance.
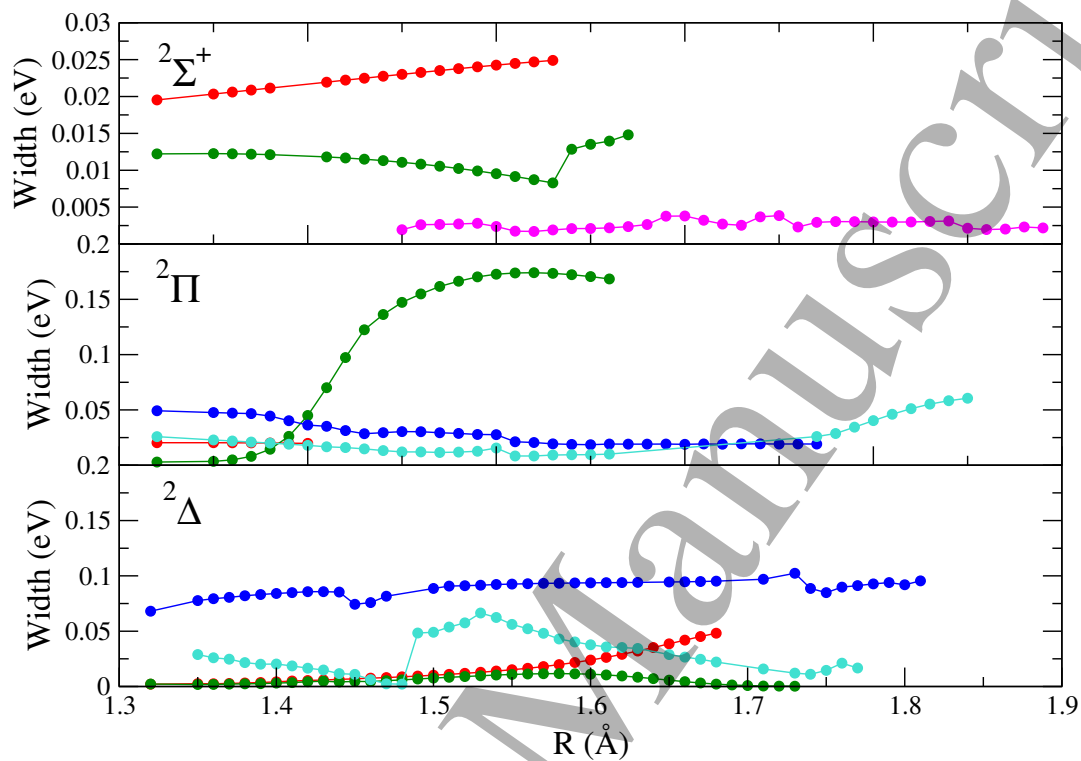
Figure 11: Resonance widths as a function of internuclear distance in agreement with the resonances from figures 8, 9, and 10. The corresponding symmetry of the resonant states is indicated in the figure.

Bound and resonant states of NS molecule   17

[1] Somerville W B 1977 *Rep. Prog. Phys.* **40**, 483.
[2] Demarçay E 1880 *Compt. Rend.* **91**, 854.
[3] Preuss K E 2007 *Dalton Trans.* **23**, 2357.
[4] Cernicharo J, *et al.* 2018 *ApJL* **853**, L22.
[5] Rivière-Marichalar P, *et al.* 2019 *A&A* **628**, A16.
[6] O'Hare P A G 1970 *J. Chem. Phys.* **52**, 2992.
[7] Török F, PuIay P, Szondy T, Nagy P 1974 *Acta Chim. Hung.* **80**, 139.
[8] Karna S P and Grein F 1986 *Chem. Phys.* **109**, 35.
[9] Ben Yaghlane S and Hochlaf M 2009 *J. Phys. B: At. Mol. Opt. Phys.* **42**, 015101.
[10] Lie G C, Peyerimoff S D and Buenker R J 1985 *J. Chem. Phys.* **82**, 2672 and references therein.
[11] Burke P G 2011 *R-Matrix Theory of Atomic Collisions* Springer: Heidelberg, Berlin.
[12] Tennyson J 2010 *Phys. Rep.* **491**, 29.
[13] Masin Z, Benda J, Gorfinkiel J D, Harvey A G and Tennyson J 2020 *Comput. Phys. Commun.* **249**, 107092.
[14] Werner H-J, Knowles P J, Knizia G, Manby F R and Schütz M 2012 *WIREs Comput Mol Sci* **2**, 242.
[15] Morgan L A, Tennyson J and Gillan C J 1998 *Computer Phys. Commun.* **114**, 120.
[16] Faure A, Gorfinkiel J D, Morgan L A and Tennyson J 2002 *Gtobas: Comput. Phys. Commun.* **144**, 224.
[17] Morgan L A 1984 *Comput. Phys. Commun.* **31**, 419.
[18] Tennyson J and Noble C J 1984 *Comput. Phys. Commun.* **33** 421.
[19] Sarpal B K, Branchett S E, Tennyson J and Morgan L A 1991 *J. Phys. B: At. Mol. Opt. Phys.* **24**, 3685.
[20] Zhang R, Baluja K L, Franz J and Tennyson J 2011 *J. Phys. B: At. Mol. Opt. Phys.* **44**, 035203.
[21] Little D A, Chakrabarti K, Mezei J Zs, Schneider I F and Tennyson J 2014 *Phys. Rev. A* bf 90, 052705.
[22] Niyonzima S, Ilie S, Pop N, Mezei J Zs, *et al.* 2017 *At. Data Nucl. Data Tables* bf 115-116, 287.
[23] Niyonzima S, Pop N, Iacob F, Larson Å, *et al.* 2018 *Plasma Sources Sci. Technol.* bf 27, 025015.
[24] Pop N, Iacob F, Niyonzima S, Abdoulanziz A, Laporta V, Reiter D, Schneider I F and Mezei J Zs 2021 *At. Data Nucl. Data Tables* **139**, 101414.
[25] Epée Epée M D, Motapon O, Pop N, Iacob F, Roueff E, Schneider I F and Mezei J Zs 2022 *MNRAS* **512**, 424.
[26] Kokoouline V, Ayouz M, Mezei J Zs, Hassouni K and Schneider I F 2018 *Plasma Sources Sci. Technol.* **27**, 115007.